ELSEVIER

15 April 1996

Optics Communications 125 (1996) 359–368

OPTICS COMMUNICATIONS

Full length article

Limitations imposed by spatial hole burning on the single-frequency performance of unidirectional ring lasers

K.I. Martin, W.A. Clarkson, D.C. Hanna

Optoelectronics Research Centre, University of Southampton, Southampton SO17 1BJ, UK

Received 9 August 1995; revised 16 October 1995; accepted 26 November 1995

Abstract

Residual spatial-hole-burning in a unidirectional ring laser can limit the maximum power available in a single-frequency. These effects have been modelled numerically and verified experimentally in Nd:YAG and Nd:YLF lasers. For convenience, an analytical expression for maximum single-frequency power has also been developed for use in designing ring lasers.

Keywords: Spatial hole-burning; Single-frequency; Diode-pumped; Ring laser

1. Introduction

The observation that spatial hole-burning causes multi-axial-mode oscillation was made in the early days of lasers [1]. Various approaches have been taken to eliminate spatial hole-burning, in order to achieve single-frequency operation, the most widely used being the unidirectional ring laser [2]. This has proved to be an extremely effective way to achieve robust single-frequency operation.

However it has to be recognised that, even in such a unidirectional laser, it is possible to have some degree of residual hole-burning, due, for example, to backward-travelling reflections from imperfect anti-reflection coatings overlapping with the forward beam in the gain medium. The presence of such a residual spatial-hole-burning can lead to the result that, at some power level of the dominant mode, oscillation of an additional axial mode, or modes, can start up. The safest remedy for avoiding this is to rigorously eliminate the spurious reflections, for example by using Brewster-angle surfaces on the laser medium, and tilting other reflective surfaces sufficiently. Ideally, also, the laser rod should be well removed from any resonator mirror, since overlap of the incident and reflected beams at the mirror is unavoidable. However this situation of overlap in the gain medium at the mirror is an inevitable feature of monolithic lasers (see e.g. Ref. [3]), and even when avoidable, as in a non-monolithic laser, it is often a matter of convenience to put one of the resonator mirrors directly on the laser medium. This particular arrangement is shown schematically in Fig. 1a, with the pump entering through the dichroic reflector. The overlap region, shown hatched in Fig. 1a, can clearly be of a much reduced extent compared to that of a typical standing-wave resonator and single-mode operation will therefore be possible to a higher-power level than in a standing-wave configuration. However at some power level, which will depend on the extent of overlap, multimode operation will occur. Typical numbers from our own experiments and from our numerical estimates indicate that where beam overlap as in Fig. 1 occurs, multimode opera-

SSDI 0030-4018(95)00710-5

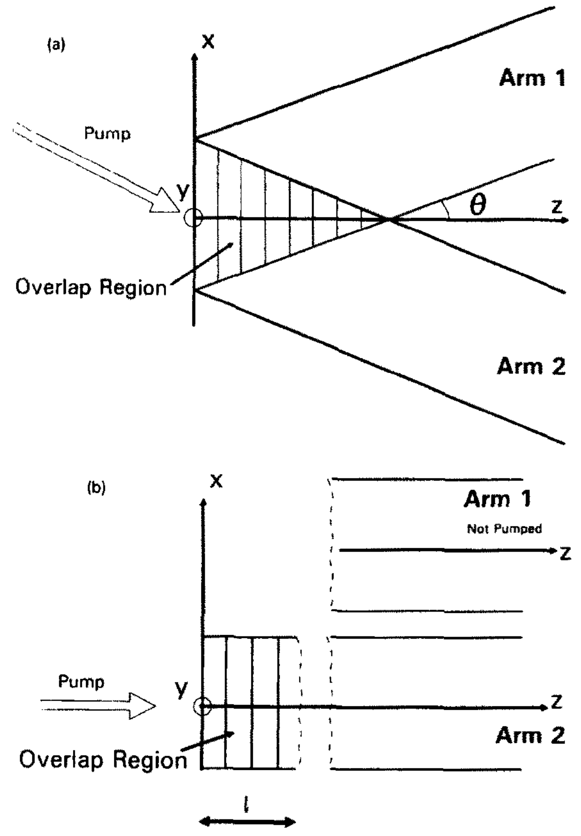

Fig. 1. Overlap diagrams for a ring laser end pumped through a dichroic coating on the surface of the laser rod. (a) The actual overlap region. (b) The equivalent overlap region in a standing wave laser, used for the analytical approximation.

tion can start in Nd:YAG in the region of a 100 mW –1 W of power. On the other hand, we have found that by separating the laser rod from the mirror, so that no overlap occurs, single-mode operation can be extended to powers of more than 5 W, and not show any evidence of multimode operation.

Thus the effects of beam overlap do become serious at the sort of power levels of current interest to laser developers. To the laser designer it is clearly important to have some ability to predict the maximum power level for single-frequency operation, and the way in which this power level is influenced by parameters that affect the overlap, such as pump beam and laser beam spot-sizes, angle of incidence, and material parameters, such as absorption length, gain linewidth, fluorescence lifetime, emission cross-section etc.

The aim of the work reported here [4] has been to develop a suitable quantitative predictive capability that can be of use to the laser designer. A theoretical treatment aimed at predicting maximum single-mode power has been developed. This quickly leads to mathematical complications so various simplifying approximations have been made to reduce the theory to an analytical result which can be readily used. To check the usefulness of this result, it has been compared with more detailed computational results, and also compared with experimental results obtained from diode-pumped Nd:YAG and Nd:YLF lasers. The approximate result is seen to give a very useful guideline to actual experimental behaviour. One result is a confirmation of the fact that Nd:YAG with its narrower gain-linewidth and hence stronger gain-discrimination between adjacent modes, allows higher single-mode power (other things being equal) than a Nd:YLF laser. (We assume here that mode selection occurs solely through the gain profile, i.e. no other frequency discrimination elements are incorporated.) The behaviour of maximum single-mode power versus angle of incidence confirms the expected increase with angle. Indeed, this predictive capability has been used in designing a monolithic Nd glass ring laser [5], ensuring that parameters were chosen to allow single-frequency operation up to the intended operating power level.

The lay out of the paper is as follows. The theory section gives a brief outline of the basis for calculating maximum single-mode power for a resonator containing an overlap region of the form shown in Fig. 1a. The algebraic details are relegated to an appendix, and only the approximate analytical expression is displayed in the theory section. Then follows a description of the experimental measurements and their comparison with prediction.

2. Theory and discussion

The analysis is confined to the steady state, starting from the rate equations with net rates of change of inversion and photon population set equal to zero. The pump mode and laser mode are assumed to have Gaussian spatial profiles. With a given pump rate per unit volume (determined by pump power, spot-size and pump absorption coefficient), and laser intensity

[redacted]

distribution, we calculate the inversion distribution in the gain medium, by finding the intracavity single frequency laser power that saturates the net-gain to unity. For this calculation the laser intensity distribution includes the standing wave behaviour in the overlap region. Such a calculation involves overlap integrals between the transverse profiles of the laser and pump modes, which in its general form leads to algebraically complicated expressions. The net gain available to other mode frequencies can then be calculated via the same overlap integrals. As lasing power in the single-mode increases, due to increased pumping, eventually a point is reached at which the net gain available to another mode reaches unity, and hence multimode oscillation commences. The goal of the calculation is to find the single-mode power level at which this onset of multimode oscillation occurs.

To simplify the analysis various approximations are made. A "low-power" approximation is made in that a binominal expansion is made of the denominator containing the gain saturation term. Computations have been made with the second order term of the binominal expansion included. However to arrive at an analytical expression, the stronger approximation was made of restricting to just the first order term. For the analytical expression a further simplification was made, by simulating the overlap region, with its complex form shown in Fig. 1a, by a simple cylindrical overlap region, of some appropriate effective length, as shown in Fig. 1b. The usefulness of this approach was confirmed by comparing with the fuller computational approach, with satisfactory agreement being obtained.

The simplified analytical result gives the maximum single-mode power, P_{sm} expressed as

$$P_{sm} = \eta P_s g, \tag{1}$$

η is a geometrical factor, dependent on the laser and pump mode spot sizes (W_{lx}, W_{ly}, W_{px}, W_{py} for the x and y transverse directions),

$$\eta = \left(\frac{2W_{px}^2 + W_{lx}^2}{W_{px}^2 + W_{lx}^2} \right)^{1/2} \left(\frac{2W_{py}^2 + W_{ly}^2}{W_{py}^2 + W_{ly}^2} \right)^{1/2}. \tag{2}$$

P_s is the saturation output power given by

$$P_s = \frac{\pi W_{lx} W_{ly} T h \nu_L}{4 \sigma \tau_f}, \tag{3}$$

where σ is the stimulated emission cross section for the laser transition, τ_f is the fluorescence lifetime, T is the transmission of the output coupler, h is Planck's constant, and ν_L is the frequency of the lasing light.

For most lasers of interest, the cavity length is much longer than the absorption length of the pump beam, and the length of the overlap region. Under these conditions, g is given by

$$g \simeq \frac{1 + \alpha_p l}{\frac{1}{6} \Delta k_L^2 n^2 \cos^2\theta \, \alpha_p l^3 + 1 + 2\alpha_p l}. \tag{4}$$

Here α_p is the pump absorption coefficient, n the refractive index of the laser medium, l is effective overlap length, Δk_L is the gain linewidth in wave numbers (FWHM). The effective overlap length l, is related to the laser spot-size W_l, and angle θ by

$$l = \frac{0.45 W_l}{\sin\theta}, \tag{5}$$

where the numerical factor 0.45 corresponds to the value for which the analytical results best fit the numerical calculation based on the first order binominal approximation.

Substituting for l, from Eq. (5) in Eq. (3) gives

$$g \sim \left[1 + \frac{0.45 \alpha_p W_l}{\sin\theta} \right] \left[\frac{n^2 \cos^2\theta \Delta k_L^2 \alpha_p}{6} \left(\frac{0.45 W_l}{\sin\theta} \right)^3 + 2 \frac{0.45 \alpha_p W_l}{\sin\theta} + 1 \right]^{-1}. \tag{6}$$

From this equation one can see the salient features of the dependence of P_{sm} on various parameters.

The expression for maximum single-mode output power, in Eq. (1) is the product of three terms. The term η, is a purely geometrical factor expressing the degree of overlap between the pump and laser modes. It does not depend strongly on the mode sizes and typical values of η are in the range 1–1.5.

The term P_s is the saturation output power, i.e. the corresponding output power when the internal circulating intensity is equal to the saturation intensity of the laser transition. Thus, as seen from the expression for P_s in Eq. (3), a large saturation intensity and a high output mirror transmission lead to a high value for the maximum single-frequency output power. However, it must be borne in mind that a high saturation and high transmission can give a high threshold, and hence a low overall efficiency. The dependence of P_s on laser spot-size, is in fact counteracted by a stronger inverse dependence on spot-size through the term g.

Of the three terms in Eq. (1), the term g has the most complicated behaviour. It accounts for the overlap between the axial modes of the cavity and the distribution of inversion. In the expression for g, in Eq. (6), the denominator is dominated by its first term. Thus one sees that the maximum single-frequency power is inversely proportional to the square of the medium's refractive index and the square of the gain linewidth. The refractive index dependence can be understood from the fact that a smaller index gives wider spacing of the nodes, and hence a greater frequency shift is needed to access the undepleted gain at the nodes of the dominant mode. The linewidth dependence reflects the fact that a broader line offers less gain discrimination between modes, hence reduced maximum single-mode power. Taking account of the relevant parameters for Nd:YAG and Nd:YLF, through P_s and g, it is found, and confirmed experimentally that Nd:YAG is the more favourable for higher single-mode power.

The dependence of g on pump absorption coefficient, α_p, arises from the fact that a large α_p means that the overlap region is a larger fraction of the absorption region, so resulting in a reduction of the maximum single-frequency power. The remaining variable in g is l, which in turn depends on W_l and θ as given in Eq. (5).

The cubed dependence on l, and hence on $\sin\theta$, implies a strong increase in maximum single-frequency power with increasing angle of incidence θ. This in fact provides the single most important factor influencing the single-mode power. The dependence on spot-size W_l, is more complicated. For the conditions under which the approximation leading to Eq. (6) are valid i.e. $\alpha l < 1$, then the W_l^{-3} dependence of g outweighs the W_l^2 dependence of P_s, so that the maximum single mode power decreases with increased spot-size. In fact, in our experiments, we have deliberately chosen a large W_l in order to reduce the power level for multimode operation to a value that could be accessed with our available pump-power. On the other hand, for linear, standing-wave, cavities, or ring cavities where θ is small, so that $\alpha l \gg 1$, then one has to use Eq. (A31) in the appendix, which for large αl becomes

$$g \approx \frac{2}{\left(n^2 \Delta k_L^2 \cos^2\theta\right)/\alpha_p^2 + 3}. \tag{7}$$

This is independent of W_l, so that the dependence of maximum single-mode power on W_l is determined by P_s, i.e. increasing spot-size gives increasing single-mode power.

One should also note that the expression for P_{sm} does not depend on cavity loss (other than through the output mirror transmission), or on the resonator length. This independence from cavity length is valid for lasers where the cavity length is much greater than the absorption length, and has previously been demonstrated by Kintz and Baer [6]. The basis of this result is that longer cavities result in smaller mode frequency differences which, while implying reduced gain discrimination in the gain line shape, also means reduced access to undepleted gain in the standing wave pattern. These two effects cancel, whereas in shorter cavities, such as micro-chip lasers, the increased gain discrimination becomes the dominant effect.

To summarise this discussion, we note that several steps can be taken to increase the maximum single-mode power, the most useful being to make θ large. The laser spot-size should be kept small and a high output transmission should be used. In choosing a material, a narrow-linewidth and low refractive index are desirable features.

We now describe some experiments aimed at verifying some of the predictions from the analysis.

3. Experiment

The goal of the experiments was to observe the dependence of single-mode power on the angle of incidence θ, so that a check could be made on agreement with the calculation. For the experiment, a ring laser was used with the configuration as shown in Fig. 2, consisting of a rhomb-shaped acousto-optic modulator crystal, having four Brewster's angle surfaces. The rhomb serves both to define the ring path and to enforce unidirectional operation [7]. Measurements were made for the 1064 nm line of Nd:YAG

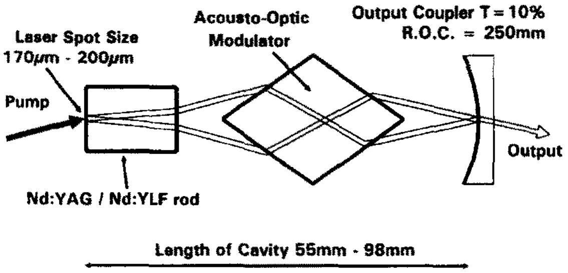

Fig. 2. Diagram of the rhomb ring laser.

and the 1053 nm line of Nd:YLF. With the Nd:YAG crystal in the resonator, the laser was pumped by two polarisation-coupled 1 W diode lasers emitting at ~ 809 nm. With Nd:YLF, only one diode laser was used, as the maximum single-frequency power of this laser is lower, so less pump power was needed to reach the onset of multi-frequency operation. This diode was operated at 796 nm. The pump beam was focused down to spot radii of approximately 80 μm (x direction) by 120 μm (y direction) using, after collimation, a set of anamorphic prisms and two cylindrical lenses. To determine the maximum single-frequency power of the laser, it is necessary to ensure that the mode-frequency is at the peak of the gain profile. This was done by scanning the resonator length, via a PZT-mounted output-mirror. The maximum single-frequency power was then found by increasing the pump power, until the output of the laser was no longer single-frequency, even when the PZT scanned the mode-frequency over the peak of the gain profile. The frequency spectrum was analyzed using a plane–plane Fabry–Perot scanning interferometer.

The angle of incidence, θ, in the gain medium, was set to various values, and measurements taken of single-frequency performance of the laser, at each θ value. The geometry of this rhomb ring laser allowed this angle to be adjusted by altering the length of the cavity i.e. by longitudinal displacement of the output mirror. This also results in changes to a number of other resonator parameters, such as the longitudinal mode spacing, the cavity loss (due to the variation of the angle of incidence at the surfaces of the rhomb), and a change in the laser mode spot-size. As the maximum single frequency power is independent of cavity loss and cavity length, and the change in the spot size is small, it is the angle θ that has the dominant effect on the maximum single-frequency power of the laser. Note that the maximum single-frequency power does not depend on the round trip cavity length, l_c, despite the dependence of the mode-frequency difference, $c/2l_c$, on l_c. The explanation for this is given earlier in the theory section. An output coupler with a 25 cm radius of curvature was used, this value being chosen to obtain a large laser mode spot-size in the gain medium, i.e. waist radii at between 170 μm and 200 μm, at the high reflecting surface of the laser rod, depending on the length of the cavity. Having a large laser spot-size helped to increase spatial-hole-burning effects (see earlier), causing a reduction in the maximum single-frequency power. This was done deliberately to ensure that the maximum single-frequency power could be reached with the pump power available, and so that the low-power approximation used in the theory is valid. Having a large spot-size also reduced any effect of the cavity length variation on the spot-size. The thresholds were approximately, for the Nd:YAG cavity, 300 mW for the shortest cavity, going up to 700 mW for the 10 cm cavity. This difference was due to the increased loss at the Brewster faces (10% round trip) and the larger laser mode spot-size.

4. Discussion of results

The results for single-mode power dependence on angle θ are shown in Fig. 3. The parameter values used in the calculations are shown in Table 1. Reported values for the emission cross section, σ, on the 1.053 μm transition in Nd:YLF vary from 1.2×10^{-23} m^2 [8] to 2.6×10^{-23} m^2 [9]. The former value gave the best agreement with our experiment. The value we have used in this paper is the most recent available, 1.4×10^{-23} m^2 [10]. The values of the constants for Nd:YAG were taken from Ref. [11]. Note that, as seen from Eq. (3), the theoretical curves plotted in Fig. 3 scale as σ^{-1}. As seen in Fig. 3 the agreement between theory and experiment is satisfactory, particularly in view of the various simplifying approximations made. The theoretical curves in Fig. 3 were obtained numerically, using the second order binominal approximation. In Fig. 4, a comparison is made between the analytical approxi-

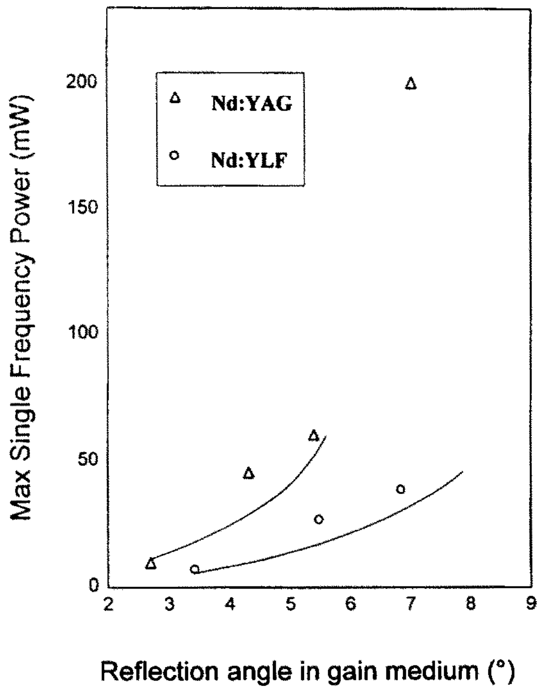

Fig. 3. A graph of maximum single frequency power against angle θ. The symbols show experimental results. The lines show the values obtained from the low power second order binomial approximation.

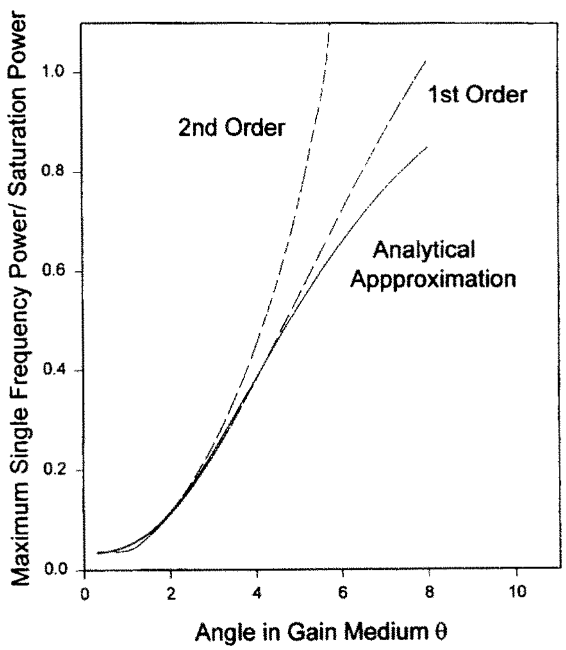

Fig. 4. A graph showing a comparison of predicted values for the maximum single frequency power of the laser, as a function of the angle of incidence, obtained using the approximate analytical expression, and the numerical first and second order approximations.

mation and the numerical calculation, both for the first order and second order approximation. Where the approximations break down the formulae give an underestimate of the maximum single-frequency power. These results show that the analytical formulae give a useful quantitative guide over much of the parameter range of interest, and allow an estimate to be made of the minimum angle required to achieve single frequency operation at a desired output power.

Table 1
Values of constants used in calculations

	Nd:YAG (1064 nm)	Nd:YLF (1053 nm)
Gain line width (GHz), FWHM	150	360
Emission cross section ($\times 10^{-23}$ m^2)	3.2	1.42
Fluorescence lifetime (μs)	230	440

The results also confirm the prediction that a greater P_{sm} on the 1.064 μm line of Nd:YAG than on the 1.053 μm line of Nd:YLF.

5. Conclusions

We have shown that a simplified analytical result gives a useful quantitative guideline for predicting the maximum single-frequency power from a ring laser where there is overlap of the counter-propagating waves in the gain medium. The analysis indicates how the maximum single-frequency power depends on the various resonator and material parameters that can be chosen by the designer. The numbers indicated by the calculation indicate that typical monolithic Nd:lasers, without deliberate design to minimise residual spatial hole-burning, would have maximum single-mode powers in the region of 1 W, but capable of being significantly enhanced with appropriate design. It should also be noted that the maxi-

[redacted]

mum single-frequency power calculated here corresponds to the mode being at line centre. For robust single-frequency operation one should downgrade the expected maximum power to allow the mode be moved away from exact line centre.

Acknowledgements

This work has been supported by the SERC. KIM is supported via an SERC CASE studentship sponsored by Lumonics Ltd. WAC acknowledges support via the SERC/DTI Link Optoelectronics scheme in a joint programme with Gooch and Housego Ltd.

Appendix A

The procedure for calculating the maximum single frequency power of a homogeneously-broadened four-level laser is as follows:

Using the same notation as in Refs. [12,13] the rate equations relating to the inversion density, $n(x, y, z)$ and the cavity photon density, $s_i(x, y, z)$ in the ith axial mode can be written as

$$\frac{\mathrm{d}n}{\mathrm{d}t}(x, y, z) = r(x, y, z) - \frac{n(x, y, z)}{\tau_f} - c_n n(x, y, z) \sum_i \sigma_i s_i(x, y, z), \tag{A1}$$

$$\frac{\mathrm{d}S_i}{\mathrm{d}t} = \int_{\text{cavity}} c_n \sigma_i n(x, y, z)\, S_i s_{i0}(x, y, z)\, \mathrm{d}V - \gamma S_i \tag{A2}$$

where

$$S_i = \int_{\text{cavity}} s_i(x, y, z)\, \mathrm{d}V \tag{A3}$$

is the total number of cavity photons in the ith axial mode, σ_i is the stimulated emission cross section for the ith axial mode, $r(x, y, z)$ is the pump rate per unit volume, c_n is the velocity of light in the laser medium, τ_f is the fluorescence lifetime and γ is the inverse of the cavity photon lifetime (assumed to be constant for all axial modes).

Under steady state operating conditions,

$$\frac{\mathrm{d}n}{\mathrm{d}t} = \frac{\mathrm{d}S_i}{\mathrm{d}t} = 0 \tag{A4}$$

the rate equations (A1) and (A2) can be written as

$$Rr_0(x, y, z) - \frac{n(x, y, z)}{\tau_f} - c_n n(x, y, z) \sum_i \sigma_i S_i s_{i0}(x, y, z) = 0 \tag{A5}$$

and

$$\int_{\text{cavity}} c_n \sigma_i n(x, y, z)\, S_i s_{i0}(x, y, z)\, \mathrm{d}V - \gamma S_i = 0 \tag{A6}$$

where R is the total pump rate, and $r_0(x, y, z)$ and $s_{i0}(x, y, z)$ are normalised distributions for pump rate per unit volume and photon density in the ith axial mode defined by

$$r(x, y, z) = Rr_0(x, y, z),$$
$$S_i(x, y, z) = S_i s_{i0}(x, y, z),$$
$$\int_{\text{cavity}} r_0(x, y, z)\, \mathrm{d}V = \int_{\text{cavity}} s_{i0}(x, y, z)\, \mathrm{d}V = 1. \tag{A7}$$

Hence from (A5) we obtain a steady-state inversion density for single-axial-mode oscillation on the highest gain ($i = 0$) axial mode given by

$$n(x, y, z) = \frac{\tau_f R r_0(x, y, z)}{1 + S_0 s_{00}(x, y, z)/I_0}, \tag{A8}$$

where

$$I_0 = 1/c_n \sigma_0 \tau_f. \tag{A9}$$

For the lasing mode ($i = 0$) Eq. (A6) becomes

$$\int_{\text{cavity}} c_n \sigma\, n(x, y, z)\, s_{10}(x, y, z)\, \mathrm{d}V = \gamma. \tag{A10}$$

For other axial modes, during single frequency operation, the number of cavity photons, S_i is zero, and Eq. (A6) becomes trivial. At the threshold of the second mode to lase (the $i = 1$ mode, say) S_1 is non zero and Eq. (A6) becomes

$$\int_{\text{cavity}} c_n \sigma\, n(x, y, z)\, s_{10}(x, y, z)\, \mathrm{d}V = \gamma. \tag{A11}$$

Combining Eqs. (A10) and (A11) and substituting for $n(x, y, z)$ using Eq. (A8) gives

$$I_1 \int_{\text{cavity}} \frac{r_0 s_{00}}{1 + S_{\text{sm}} s_{00}/I_0} \, \mathrm{d}V = I_0 \int_{\text{cavity}} \frac{r_0 s_{10}}{1 + S_{\text{sm}} s_{00}/I_0} \, \mathrm{d}V, \tag{A12}$$

where S_{sm} is the maximum number of cavity photons before a second mode reaches threshold, and the laser becomes multi-frequency. The maximum single-frequency output power of the laser can then be written as:

$$P_{\text{sm}} = ch\nu_0 T S_{\text{sm}}/l_c, \tag{A13}$$

where c is the speed of light in vacuo, h is Planck's constant, ν_0 is the frequency of the lasing mode, T is the transmission of the output coupler of the laser, and l_c is the round trip optical length of the cavity.

In the low power limit, $S_{\text{sm}} s_{00}/I_0 \ll 1$, using a binomial expansion of the denominator, Eq. (A12) can be simplified. In order to obtain the numerical results presented in this paper, a second order binomial expansion was used. However, to obtain an analytical result, we have kept only terms to first order, to give the following approximate expression for S_{sm}

$$S_{\text{sm}} = \frac{I_0 (I_1 - I_0) \int r_0 s_{00} \, \mathrm{d}V}{I_1 \int r_0 s_{00}^2 \, \mathrm{d}V - I_0 \int r_0 s_{00} s_{10} \, \mathrm{d}V}. \tag{A14}$$

We are interested here in the case of a ring cavity which is end pumped through one surface of the gain medium, which is also totally reflecting at the lasing wavelength. This means that there is a region adjacent to the high reflector where the incident and reflected beams overlap (see Fig. 1a). Solving Eq. (A14) for this complicated overlap cannot be done analytically. So, for the analytical solution, we simplify by treating this situation as a linear cavity, where the overlap occurs in a cylindrical region, over some effective distance l into the gain medium. The effective length l will depend on θ, the angle of incidence of the laser mode on the gain medium surface, and on the beam spot size, W_l.

For a linear cavity,

$$r_0(x, y, z) = \frac{2\alpha_p}{\pi W_{px} W_{py} (1 - \mathrm{e}^{-\alpha_p l_g})} \times \exp\left[-\left(\frac{2x^2}{W_{px}^2} + \frac{2y^2}{W_{py}^2} + \alpha_p z \right) \right], \tag{A15}$$

where l_g is the length of the laser medium, α is the absorption coefficient for the pump, and W_{px} and W_{py} are the pump spot sizes in the x and y dimensions respectively. The normalised photon density s_{i0} is given by,

$$s_{i0}(x, y, z) = \frac{2nf_i(z)}{\pi W_{lx} W_{ly} L} \exp\left[-\left(\frac{2x^2}{W_{lx}^2} + \frac{2y^2}{W_{ly}^2} \right) \right], \tag{A16}$$

where W_{lx} and W_{ly} are the laser mode spot sizes, in the x and y directions respectively, n is the refractive in the gain medium, and

$$\left.\begin{aligned} f_0(z) &= 2\sin^2(k_0 nz\cos\theta) \\ f_1(z) &= 2\sin^2(k_1 nz\cos\theta) \end{aligned}\right\} z \le l \qquad \left.\begin{aligned} f_0(z) &= 1 \\ f_1(z) &= 1 \end{aligned}\right\} z > l \tag{A17}$$

k_0 and k_1 are the wave numbers in air for the $i = 0$ and $i = 1$ axial modes respectively.

Eq. (A14) then becomes

$$S_{\text{sm}} = \frac{\pi W_{lx} W_{ly} L \eta g I_0}{2}, \tag{A18}$$

where

$$\eta = \left(\frac{2W_{px}^2 + W_{lx}^2}{W_{px}^2 + W_{lx}^2} \right)^{1/2} \left(\frac{2W_{py}^2 + W_{ly}^2}{W_{py}^2 + W_{ly}^2} \right)^{1/2}, \tag{A19}$$

and

$$g = \frac{(I_1 - I_0) \int_0^{l_g} f_0(z) \mathrm{e}^{-\alpha z} \mathrm{d}z}{I_1 \int_0^{l_g} f_0^2(z) \mathrm{e}^{-\alpha z} \mathrm{d}z - I_0 \int_0^{l_g} f_0(z) f_1(z) \mathrm{e}^{-\alpha z} \mathrm{d}z}. \tag{A20}$$

Geometrical considerations suggest that an appropriate value for l would be

$$l = \frac{W_l}{2\sin\theta}. \tag{A21}$$

The maximum single frequency output power can now be written as

$$P_{sm} = P_s \eta g, \tag{A22}$$

where P_s is the saturation output power:

$$P_s = \frac{\pi W_{lx} W_{ly} T h \nu_0}{4 \sigma \tau_f}. \tag{A23}$$

The low power approximation condition then becomes:

$$P_{sm} \ll P_s. \tag{A24}$$

For a homogeneously broadened transition, with a Lorentzian line shape, we define a quantity ρ,

$$\rho \equiv \frac{I_0}{I_1} = \frac{\sigma_0}{\sigma_1} \simeq 1 + \frac{4\Delta\nu^2}{\Delta\nu_L^2} = 1 + \frac{4\Delta k^2}{\Delta k_L^2}, \tag{A25}$$

where $\Delta\nu_L$ is the frequency line width (FWHM), Δk_L is the linewidth in wave numbers in vacuo, $\Delta\nu$ is the frequency separation between the lasing mode and the next mode to lase, and Δk is the separation in wave numbers, in vacuo:

$$\Delta k = \frac{2\pi\Delta\nu}{c}. \tag{A26}$$

Carrying out the integration in Eq. (A20) gives

$$g = \frac{(\rho - 1)(2 - e^{-\alpha_p l_s})}{3\rho - 2 + (1 - 2\rho) e^{-\alpha_p l} + (\rho - 1) e^{-\alpha_p l_s} - \alpha_p I}, \tag{A27}$$

where

$$I = \left[2\Delta kn \cos\theta \sin(2\Delta knl \cos\theta)\, e^{-\alpha_p l} + \alpha_p - \alpha_p \cos(2\Delta knl\cos\theta)\, e^{-\alpha_p l}\right] \times \left(4\Delta k^2 n^2 \cos^2\theta + \alpha_p^2\right)^{-1}. \tag{A28}$$

In order simplify this equation, several approximations can be made. If it is assumed that all the pump is absorbed in the gain medium, and assuming that $l \ll L$ (i.e. in the overlap region $2\Delta knl \cos\theta \ll \pi$) so that then the following expression for g can be written.

$$\sin(2\Delta knl\cos\theta) \simeq 2\Delta knl\cos\theta,$$

$$\cos(2\Delta knl\cos\theta) \simeq 1 - \frac{(2\Delta knl\cos\theta)^2}{2}, \tag{A29}$$

$$g = \left[(2 - e^{-\alpha_p l})\left(4\Delta k^2 n^2 \cos^2\theta + \alpha_p^2\right)\right] \times \left\{\left(4\Delta k^2 n^2 \cos^2\theta + \alpha_p^2\right)(3 - 2e^{-\alpha_p l}) + \Delta k_L n^2 \times \cos^2\theta \left[1 - \left(1 + \alpha_p l + \alpha_p^2 l^2/2\right) e^{-\alpha_p l}\right]\right\}^{-1}. \tag{A30}$$

For most lasers of interest the cavity length is much greater than the absorption length for the pump and hence $\Delta k \ll \alpha_p$. Under these circumstances Eq. (A30) for g can be approximated to

$$g \simeq \frac{(2 - e^{-\alpha_p l})}{(\Delta k_L^2 n^2 \cos^2\theta)/\alpha_p^2} \times \frac{1}{\left[1 - \left(1 + \alpha_p l + \alpha_p^2 l^2/2\right) e^{-\alpha_p l}\right] + 3 - 2e^{-\alpha_p l}}. \tag{A31}$$

Now it can be seen that the maximum single frequency power is independent of the axial mode spacing. The physical explanation for this is that for a mode with a large frequency spacing from the lasing line will have its low stimulated emission cross section compensated for by its good overlap with the inversion distribution.

Further simplification of the expression for g can be made if one makes the additional assumption that the pump absorption length is significantly longer than the overlap length, (i.e $\alpha_p l \ll 1$). Care must be taken with this approximation as in the first term in the denominator of Eq. (A31), terms to third order in $\alpha_p l$ need to be retained, as the first and second order components cancel out. The third order term is multiplied by a large constant, so it cannot be neglected. For example, if the laser medium is Nd:YAG, this constant is,

$$\frac{n^2 \Delta k_l^2}{\alpha_p^2} \simeq 2 \times 10^2. \tag{A32}$$

Eq. (A31) then becomes

$$g = \frac{1 + \alpha_p l}{\frac{1}{6}\left(\Delta k_L^2 n^2 \cos^2\theta\right) \alpha_p l^3 + 2\alpha_p l + 1}. \tag{A33}$$

This is the expression on which the discussion in the theory is based.

References

[1] C.L. Tang, H. Statz and G. de Mars, J. Appl. Phys 34 (1963) 2289.

[redacted]

[2] A.E. Siegman, Lasers (University Science Books, Mill Valley, CA, USA, 1986) pp. 532–538.
[3] T.J. Kane and R.L. Byer, Optics Lett. 10 (1985) 65.
[4] K.I. Martin, W.A. Clarkson and D.C. Hanna, in: Advanced Solid State Lasers, OSA Proceedings Series, Vol. 20 (Optical Society of America, Washington, D.C., 1994) p. 269.
[5] C. Bollig, W.A. Clarkson, D.C. Hanna, D.S. Lovering, and G.C.W. Jones, in: Conf. on Lasers and Electro-Optics, Vol. 15, OSA Technical Digest Series (Optical Society of America, Washington, D.C., 1995) p. 124.
[6] G.J. Kintz and T. Baer, IEEE J. Quantum Electron. 26 (1990) 1457.
[7] W.A. Clarkson and D.C. Hanna, Optics Comm. 81 (1991) 375.
[8] T.M. Pollak, W.F. Wing, R.J. Grasso, E.P. Chicklis and H.P. Jenssen, IEEE J. Quantum Electron. 18 (1982) 159.
[9] N.P. Barnes, D.J. Gettemy, L. Esterowitz and R.R. Allen, IEEE J. Quantum Electron. 23 (1987) 1434.
[10] A.L. Harmer, A. Linz and D.R. Gabbe, J. Phys. Chem. Solids 30 (1968) 1483.
[11] H.G. Danielmeyer, Lasers, Vol. 4, eds. A.K. Levine and A. De Maria (Marcel Dekker, New York, 1975) pp. 24–28.
[12] K. Kubodera and K. Otsuka, J. Appl. Phys. 50 (1979) 653.
[13] W.A. Clarkson and D.C. Hanna, J. Modern Optics 36 (1989) 483.